



Competition and Natural Selection in a Mathematical Model of Cancer

JOHN D. NAGY

Department of Biology,
Scottsdale Community College,
9000 E. Chaparral Road,
Scottsdale, AZ 85256-2626,
USA

E-mail: john.nagy@sccmail.maricopa.edu

A malignant tumor is a dynamic amalgamation of various cell phenotypes, both cancerous (parenchyma) and healthy (stroma). These diverse cells compete over resources as well as cooperate to maintain tumor viability. Therefore, tumors are both an ecological community and an integrated tissue. An understanding of how natural selection operates in this unique ecological context should expose unappreciated vulnerabilities shared by all cancers. In this study I address natural selection's role in tumor evolution by developing and exploring a mathematical model of a heterogeneous primary neoplasm. The model is a system of nonlinear ordinary differential equations tracking the mass of up to two different parenchyma cell types, the mass of vascular endothelial cells from which new tumor blood vessels are built and the total length of tumor microvessels. Results predict the possibility of a hypertumor—a focus of aggressively reproducing parenchyma cells that invade and destroy part or all of the tumor, perhaps before it becomes a clinical entity. If this phenomenon occurs, then we should see examples of tumors that develop an aggressive histology but are paradoxically prone to extinction. Neuroblastoma, a common childhood cancer, may sometimes fit this pattern. In addition, this model suggests that parenchyma cell diversity can be maintained by a tissue-like integration of cells specialized to provide different services.

© 2003 Society for Mathematical Biology. Published by Elsevier Ltd. All rights reserved.

1. INTRODUCTION

Malignant tumors contain two distinct cell populations: cancer cells themselves (parenchyma); and reactive stroma containing healthy cells largely subjugated by the parenchyma. Neither population is simple. For example, stroma typically contains vascular endothelial cells (VECs), pericytes and smooth muscle cells in its blood vessels (Folkman *et al.*, 2000), along with fibroblasts and other cell types characteristic of healing wounds (Weinert, 1997; Rowley, 1998; Tuxhorn *et al.*, 2001). Parenchyma cells in a given tumor, although typically derived from a single progenitor cell, also tend to show considerable phenotypic variation. To cite just

one example, most malignant lung tumors contain cells of more than one histological type, and even individual cells can exhibit features of more than one type (Mabry *et al.*, 1996). Such diversity probably results from genotypic instability characteristic of most, if not all, cancer cells (Loeb, 1996; Testa, 1996; Cheng and Loeb, 1997; Cahill *et al.*, 1999; Qumsiyeh and Li, 2001; Bertuzzi *et al.*, 2002).

This situation makes for an interesting ecology. On one hand, stromal cells integrate their activities with the parenchyma. For example, VECs build blood vessels supplying nutrients to proliferating parenchyma cells, and stromal fibroblasts secrete proteases facilitating parenchymal invasion of surrounding tissue (Terada *et al.*, 1996; Chang and Werb, 2001). On the other hand, all cells within the tumor compete for oxygen, reduced organic compounds, waste-removal services and space. In addition, stromal immune effector cells act like predators, destroying parenchyma cells and other stromal support structures like blood vessels (Colombo *et al.*, 1996). Therefore, a malignant tumor's organization is somewhere between an integrated tissue and an ecological community.

Two questions arise at this point. First, what allows for parenchyma diversity and the tissue-like organization among parenchymal and stromal subpopulations? The second question is related to the first: how will the parenchyma population evolve over time? If tumors act like ecological communities, then cell types should segregate into distinct niches and live off different sets of resources because of competitive exclusion. However, if tumors are more like integrated tissues, natural selection should favor diverse but cooperative cell types.

These questions have clinical relevance. Understanding how cells coordinate to form viable tumors generates insight into how such integration is most easily disrupted. Efforts to destroy cancers by inhibiting angiogenesis provides an example. Also, since cell composition generates a tumor's gross phenotype, elucidating how natural selection operates in a given tumor may yield techniques to alter that phenotype in the patient's favor.

Here I address these questions with a mathematical model that describes three aspects of a single solid tumor: change in mass over time; change in tumor vascularization over time; and competition between two different parenchyma cell types. In addition, since mature blood vessels arise from activated, immature VECs, a process that takes some time (Neufeld *et al.*, 1999), the model also follows the mass of immature VECs from which blood vessels are built.

Analysis of this model indicates that natural selection always favors more aggressive parenchyma cell phenotypes. That is, if a mutant cell type becomes established within the tumor, and that cell type applies more resources to reproduction than residents do, then the mutant type will tend to invade, eventually become established within and often dominate the tumor. But its doing so can alter the local environment such that a slower-growing tumor results. In fact, selection can favor phenotypes that eventually destroy part or perhaps all of the tumor, a situation which I refer to as a hypertumor. This hypertumor mechanism may be a cause of the necrosis observed in many vascularized tumors. In addition, natural selection can

create heterogenous tumors that superficially appear as a tissue-like integration of diverse parenchyma cell types. However, this integration possesses more characteristics of parasitism than cooperation. Therefore, this model supports the notion that heterogenous tumors are more like ecological systems than integrated tissues.

2. THE MODEL

Let $x_1(t)$ and $x_2(t)$ be the mass (in g) at time t of parenchyma cells with phenotypes 1 and 2, respectively. Furthermore, let $y(t)$ be the mass (g) of immature VECs within the tumor and $z(t)$ be the length of existing tumor microvessels. I scale z such that one unit is equal to the mean microvessel length in 1 gram of undiseased tissue.

The model I wish to consider is the following:

$$\left\{ \begin{array}{l} \frac{dx_1}{dt} = \Phi_1(v)x_1, \\ \frac{dx_2}{dt} = \Phi_2(v)x_2, \\ \frac{dy}{dt} = (\alpha H(x_1, x_2, z) - \beta)y, \\ \frac{dz}{dt} = \gamma y - \delta vz, \\ v(t) = \frac{z}{x_1 + x_2}, \\ H(x_1, x_2, z) = \frac{x_1 h_1(v) + x_2 h_2(v)}{x_1 + x_2}. \end{array} \right. \quad (1)$$

The variable $v(t)$ represents tumor vascularization (perfusion) in microvessel units per gram of parenchyma. To a physiologist, v is proportional to tumor microvessel length density (Weibel, 1984).

Functions $\Phi_i(v)$ express per capita growth rate of cell type i as a function of blood supply. For both biological and mathematical reasons Φ should be continuous, at least one-time differentiable and monotonically increasing with v since in general more blood means more proliferation and less death. However, Φ should approach a fixed maximum as v gets large since both cell reproduction rates and oxygen concentration within a vascularized tumor have upper limits. Also, there should be a unique, nonzero ‘break even’ perfusion where cell mortality is exactly balanced by reproduction; that is, $\Phi(v_0) = 0$ for a unique v_0 .

Functions $h_i(v)$, which I assume are continuous, positive and at least once differentiable, represent strength of an abstract angiogenesis signal emitted by tumor cells. This signal is a complex mix of pro- and anti-angiogenic growth factors secreted from and expressed on both parenchymal and stromal cells (Carmeliet and Jain, 2000; Yancopoulos *et al.*, 2000; Lobov *et al.*, 2002). Since biological details

of this signal are not completely worked out, I make the following broad assumptions based on what is known. First, as perfusion goes to zero, the signal strength also goes to zero because hypoxic cells lack energy to synthesize and release angiogenic growth factors (Kraggerud *et al.*, 1995). However, genes for certain important angiogenic signaling molecules, including vascular endothelial growth factor (VEGF), basic fibroblastic growth factor (bFGF) and platelet-derived growth factor (PDGF- β), appear to have a mechanism that allows their expression even when hypoxia becomes severe (Stein *et al.*, 1995; Miller *et al.*, 1998). Therefore, $\dot{h}(0)$ is expected to be large. On the other end, $h_i(v) \rightarrow 0$ as $v \rightarrow \infty$ because cells flush with oxygen stop producing tumor angiogenesis factors (Holash *et al.*, 1998). I also assume that $h_i(v)$ has a unique maximum that it approaches monotonically from either side.

VECs proliferate at a rate proportional to the ‘mean’ signal strength throughout the tumor, denoted $H(x_1, x_2, z)$, with proportionality $\alpha > 0$.

Parameter $\beta > 0$ describes the per capita VEC disappearance rate. VECs disappear by either dying or incorporating themselves into a growing blood vessel. I assume that the proportions in each category are fixed. Furthermore, new microvessels arise only from activated VECs at rate $\gamma > 0$ per unit mass of VECs.

In actual tumors, microvessel remodelling occurs continuously, but again the details are unclear (Colombo *et al.*, 1996; Holash *et al.*, 1998; Vajkoczy *et al.*, 2002). However, the following mechanism is a reasonable hypothesis, which I use to describe how microvessels are remodelled in model (1). First, tumors actively maintain their vascular net by secreting certain growth factors, like ang-1 (Holash *et al.*, 1998) and VEGF (Neufeld *et al.*, 1999) even after that net has been constructed. I view these growth factors as resources over which tumor cells compete. Space is another potentially limiting resource, and perhaps there are others unknown at this time, but the existence of such resources is implied by the fact that tumor vessels regress when the tumor does (Colombo *et al.*, 1996; Holash *et al.*, 1998).

Suppose one could quantify both the quantity and quality of these resources as a single real number R . Then it makes sense that R would be proportional to tumor mass, $x_1 + x_2$. Again, this conclusion is supported by the disappearance of vessels in regressing and necrotic tumors. In the model I assume that microvessels are lost at a rate proportional to the ratio z/R , say $c_1 z/R$. But, since $R = c_2(x_1 + x_2)$, per capita death rate of microvessels is δv , where $\delta = c_1/c_2$.

When we need a particular realization of the parenchyma growth function, Φ , I will use

$$\Phi_i(v) = \frac{A_i C^{p_i}}{\hat{c}_{i1}^{p_i} + C^{p_i}} - B_i \left(1 - \frac{\sigma_i C^{q_i}}{\hat{c}_{i2}^{q_i} + C^{q_i}} \right), \quad (2)$$

where $C = C(v)$ represents tumor oxygen partial pressure (P_{O_2} , measured in mmHg). Values for parameters A_i , B_i , σ_i , \hat{c}_{i1} , \hat{c}_{i2} , p_i and q_i can be obtained empirically (see Section 3). Equation (2) is similar to the model of Gammack *et al.* (2001) [see also Thompson and Royds (1999)] except for the lack of a logistic

crowding term omitted here because model (2) is meant to express dynamics of a small tumor for which exponential growth is a sufficient approximation.

The dependence of oxygen concentration on vascularization is assumed to be

$$C(v) = \frac{C_m v}{k + v}, \quad (3)$$

where C_m is the (constant) maximum P_{O_2} possible in a patient's tissues, determined primarily by the respiratory system's physiological status and the external oxygen pressure. Parameter k measures how quickly P_{O_2} responds to changes in perfusion. If $C(v)$ is expressed as partial pressure, C_m should be approximately 95 mmHg, a standard textbook value for arterial P_{O_2} under normal conditions (Weibel, 1984; Ganong, 1999). Also, given the scaling of z , when $v = 1$, tumor P_{O_2} should be about 40 mmHg (Weibel, 1984; Ganong, 1999). Therefore, $k \approx 1.375$, a result obtained by solving (3) for k when $v = 1$. Function Φ_i is now fully characterized in terms of v .

I model the angiogenesis signal produced by type i parenchyma cells as follows:

$$h_i(v) = r_i C e^{-\xi_i C}, \quad (4)$$

where $C = C(v)$ is defined by relation (3). Parameter r_i is a rough measure of a type i cell's commitment to producing the angiogenesis signal, and ξ_i roughly expresses how this commitment is affected by changes in oxygen supply.

3. PARAMETERIZATION

The fact that many key biological details are still poorly understood makes it very difficult to accurately parameterize this model. Therefore, one should view it as an early approximation that suggests dynamical possibilities; it certainly cannot be used as a predictive clinical tool. Nevertheless, for almost all parameters one can estimate at least their order of magnitude.

Perhaps the best understood parameters are those associated with the growth functions Φ_i . Thompson and Royds (1999), using data from Graber *et al.* (1996), estimated parameter values for the function Φ for two different cancer cell lines in culture—a 'wild-type' and a mutant that under-expresses *p53* (Table 1). These values, also used by Gammack *et al.* (2001), suggest that tumor cells are remarkably insensitive to changes in oxygen availability and therefore vascularization [see Fig. 2(a)]. However, given that these measurements were made on cells *in vitro*, parameters A and B in Table 1 are likely to represent upper limits for cells *in vivo*. Similarly, both \hat{c}_1 and \hat{c}_2 in Table 1 are probably lower bounds; indeed, substantial increases in either one, up to say 10 or more, have little effect on the overall form of the functions and may represent more realistic behavior *in vivo*.

Table 1. Parameter values for the parenchyma growth function Φ for two cancer cell lines. From Gammack *et al.* (2001) and Thompson and Royds (1999). Values for \hat{c} have been converted from percent to mmHg.

Cell line	A (g/day)	B (g/day)	\hat{c}_1 (mmHg)	\hat{c}_2 (mmHg)	σ	p	q
Wild-type	0.053 85	0.053 31	0.76	0.4	1.0029	2	2
<i>p53</i> mutant	0.053 85	0.026 67	0.53	0.095	1.0029	2	2

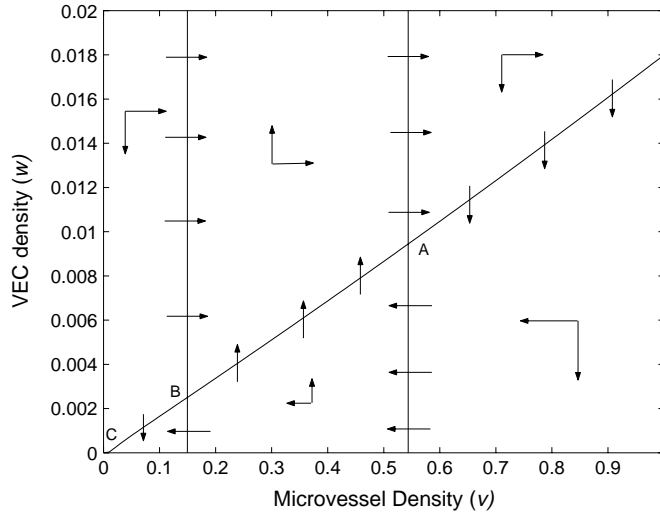


Figure 1. Nullclines and direction of flow in a typical example of model (7). In this case, $\Phi(v)$ and $h(v)$ are modelled using equations (4) and (6) with the following parameters: $A = 0.05$, $B = 0.05$, $\hat{c}_1 = 0.8$, $\hat{c}_2 = 0.4$, $\sigma = 1$, $p = q = 2$, $r = 0.28$, $\xi = 0.06$, $\alpha = 0.06$, $\beta = 0.04$, $\gamma = 3$ and $\delta = 0.004$. In this case there are four fixed points: (1) a saddle at the origin; (2) a locally asymptotically stable node at the intersection of the v nullcline with the horizontal axis (point C); (3) a saddle at point B; and (4) a locally asymptotically stable node at point A. Compare to Fig. 2, panels (c) and (d).

Precise values for the main model parameters, α , β , γ and δ , are more difficult to obtain directly. However, reasonable values may be estimated. For example, α should be the same order of magnitude as the maximal parenchyma cell growth rate A , or perhaps slightly higher since parenchyma growth rates appear to be hindered by their chromosomal instability. Therefore, in applications I set α at 0.06 as an upper limit.

The value of β is not easily available in the literature as such measurements are very difficult to make. However, as a first approximation I assume that β is on the same order of magnitude as the maximal death rate of parenchyma cells B . Therefore, I set $\beta = 0.04$ in the applications below.

If one assumes that immature and mature VECs have the same density and volume, then the parameter γ can be decomposed into the product of β and a factor,

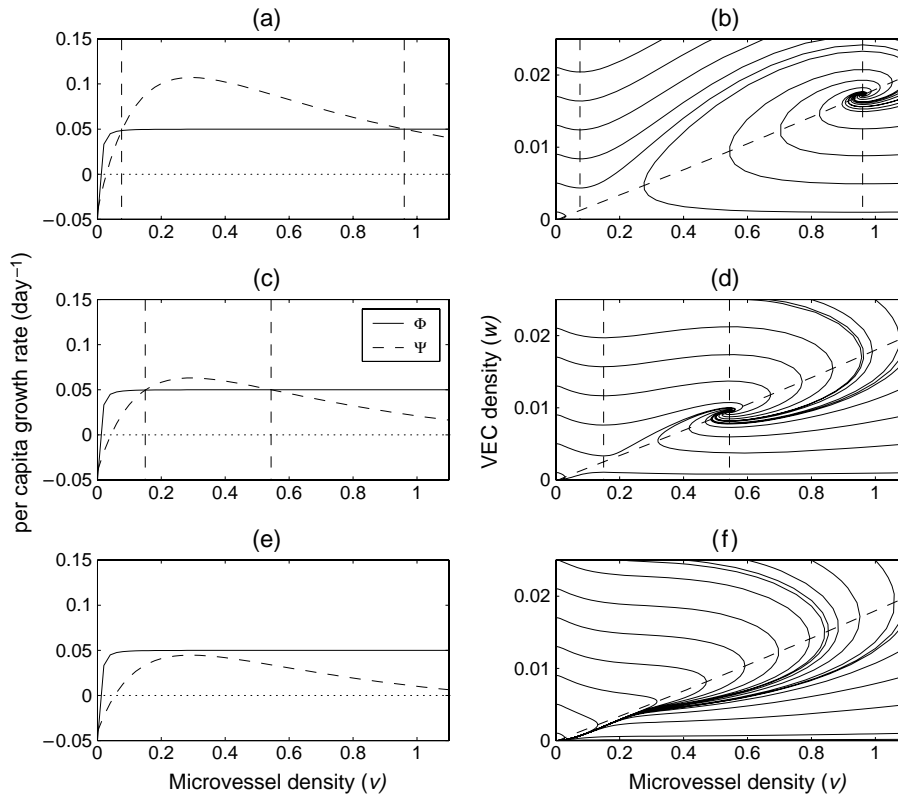


Figure 2. Three examples of the potential behavior of a homogeneous tumor [model (7)]. Left-hand panels show the relationship between the per capita growth rate of parenchyma cells (Φ , solid lines) and per capita growth rate of VECs (Ψ , dashed lines). Interior fixed points may exist where $\Phi = \Psi$, shown as vertical dashed lines in all panels. Right-hand panels are phase portraits of the model corresponding to the left-hand panels. In panels (a) and (b), $A = 0.05, B = 0.05, \hat{c}_1 = 0.8, \hat{c}_2 = 0.4, \sigma = 1, p = q = 2, r = 0.4, \xi = 0.06, \alpha = 0.06, \beta = 0.04, \gamma = 3$ and $\delta = 0.004$. In subsequent rows, r has been decreased to 0.28 [panels (c) and (d)] and 0.23 [panels (e) and (f)]; all other parameters are unchanged. This figure represents three points along the horizontal axis of the bifurcation diagram of Fig. 3.

say $\hat{\gamma}$, that converts the mass of VECs into microvessel length units. One can estimate $\hat{\gamma}$ from the literature as follows. In one biometrical study of dog blood vessel microanatomy, Horn *et al.* (1988) measure between 17 and 22 VECs per 100 μm of microvessel length. In the same paper these researchers show that endothelial cell volume is between 201 and 323 μm^3 . Assuming that VECs are approximately the same density as water, these measurements equate to about 3.5 to 7 ng of VECs per 100 μm of microvessel, which puts $\hat{\gamma}$ between 14 and 30 $\mu\text{m ng}^{-1}$. In a study of androgen-dependent tumors in rats, Jain *et al.* (1998) measured surface microvascular density in unmanipulated rats to be between 100 and 130 cm cm^{-2} . Squaring these values gives a reasonable lower bound first approximation of the

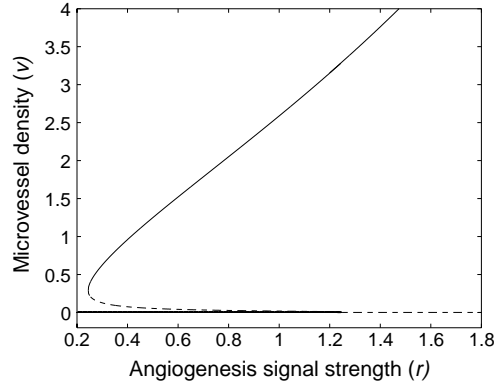


Figure 3. Local bifurcation diagram for microvessel density (v) in a homogeneous tumor [model (7)] where angiogenesis signal strength (r) is the bifurcation parameter. Other parameters are identical to those in Fig. 2. Solid lines indicate local asymptotic stability, dashed lines instability.

three-dimensional microvessel density throughout the tumor, making one unit of microvessels as scaled in the model on the order of 10^8 to perhaps $10^9 \mu\text{m g}^{-1}$. Therefore, $\hat{\gamma}$ is estimated to be between 14 and 300 microvessel units g^{-1} of VECs, placing γ between 0.56 and 12 microvessel units g^{-1} of VECs per day when $\beta = 0.04$. In the applications below I set $\gamma = 3$.

Like β , the microvessel remodelling rate δ is hard to measure, and therefore dynamical measurements are lacking in the literature. Given this situation I make the broad assumption that in normal tissue ($v = 1$) the average life expectancy of one unit of microvessels is between 1/2 and 1 year. This assumption yields an estimate of δ between 0.003 and 0.005. In the applications below I assume $\delta = 0.004$.

The most difficult parameters to estimate are those associated with h_i , the angiogenesis signal strength of cell type i . In applications, therefore, these parameters, namely r and ξ , are estimated based on the form of h . In particular, the peak signal strength should be set such that the resulting maximal VEC growth rate is of the same order of magnitude as the maximal parenchyma growth rate A . Also, as a first approximation I assume a value of ξ such that the peak VEC growth rate occurs at a vascularization of between 5 and 40% of normal [see Fig. 2(a)].

4. HOMOGENEOUS TUMOR

Before attacking the full model, it is instructive to study the special case of a tumor with only one parenchyma cell type. To that end, set $x_2(0) = 0$, which transforms model (1) into

$$\begin{cases} \frac{dx}{dt} = \Phi(v)x, \\ \frac{dy}{dt} = \Psi(v)y, \\ \frac{dz}{dt} = \gamma y - \delta vz, \\ v = \frac{z}{x}, \end{cases} \tag{5}$$

where $\Psi(v) = \alpha h(v) - \beta$, and subscripts and time dependencies are suppressed. Also, equation (2) reduces to

$$\Phi(v) = \frac{AC^p}{\hat{c}_1^p + C^p} - B \left(1 - \frac{\sigma C^q}{\hat{c}_2^q + C^q} \right). \tag{6}$$

Relation (3) is unaltered.

Since a massless tumor is undefined in this model and uninteresting in general, throughout this paper I always assume that $x(0) > 0$. Therefore, $v(t)$ is mathematically well defined at all finite times.

4.1. A simplification of model (5). The analysis of model (5) is greatly simplified by substituting $w(t) = y(t)/x(t)$ and $v(t) = z(t)/x(t)$ and differentiating to obtain the planar system,

$$\frac{dv}{dt} = \gamma w - v(\Phi(v) + \delta v), \quad \frac{dw}{dt} = (\Psi(v) - \Phi(v))w. \tag{7}$$

Here, w represents tumor VEC density (in units g of VECs/g of tumor), and v still means tumor microvessel density. If $v(0)$ and $w(0)$ and the initial parenchyma mass, $x(0)$, are known, then model (7) contains all the biological information we need about tumors obeying model (5).

Model (7) always has two boundary fixed points: the origin and $(\tilde{v}, 0)$ where \tilde{v} satisfies $\Phi(\tilde{v}) + \delta\tilde{v} = 0$. In addition, there may be any number of interior fixed points, including none. At any interior equilibrium, $v = \hat{v}$ where \hat{v} satisfies $\Phi(\hat{v}) = \Psi(\hat{v})$ (Figs. 1 and 2). At such a fixed point, $v = \hat{v}$, $w = \gamma^{-1}\hat{v}(\Phi(\hat{v}) + \delta\hat{v})$. However, the reverse implication is not true: if $\Phi(\hat{v}) = \Psi(\hat{v})$, then there may still be no interior fixed points relevant to the model. Fig. 1 shows the nullclines and general flow of a typical instance of model (7) with two interior fixed points.

The origin is either a saddle or an unstable node, as can easily be seen from the Jacobi matrix at that point:

$$\begin{pmatrix} -\Phi(0) & \gamma \\ 0 & \Psi(0) - \Phi(0) \end{pmatrix}. \tag{8}$$

Since by assumption $\Phi(0) < 0$, the larger of the two eigenvalues of matrix (8) is always strictly positive. It becomes a saddle whenever $\Psi(0) < \Phi(0)$ since

$\Psi(0) < 0$; if the inequality is reversed, then it becomes an unstable node. I ignore the biologically unlikely event that $\Psi(0) = \Phi(0)$.

The other boundary fixed point, which I will call the nontrivial boundary equilibrium, may be either locally asymptotically stable or a saddle. At this fixed point the Jacobi matrix becomes

$$\begin{pmatrix} -[\tilde{v}(\delta + \dot{\Phi}(\tilde{v}))] & \gamma \\ 0 & \Psi(\tilde{v}) - \Phi(\tilde{v}) \end{pmatrix} \quad (9)$$

since $\Phi(\tilde{v}) + \delta\tilde{v} = 0$. Therefore, the first eigenvalue is always negative because we assume $\dot{\Phi}$ is everywhere positive. So, if $\Psi(\tilde{v}) > \Phi(\tilde{v})$, then the fixed point is a saddle. If the inequality is reversed it becomes a locally asymptotically stable node. Again, I ignore the $\Psi(\tilde{v}) = \Phi(\tilde{v})$ case.

The main result describing the behavior of a homogeneous tumor is contained in the following:

PROPOSITION 1. *Suppose at least one interior fixed point exists. Then the fixed point associated with the largest \hat{v} is locally asymptotically stable. If there are an even number of interior fixed points, then exactly half are locally asymptotically stable, half are saddles and the nontrivial boundary equilibrium is a locally asymptotically stable node. If there are an odd number of interior fixed points, say n , then exactly $(n + 1)/2$ are locally asymptotically stable and the remaining $(n - 1)/2$ are saddles, as is the nontrivial boundary equilibrium.*

At any interior equilibrium the Jacobi matrix becomes

$$\begin{pmatrix} -[\Phi(\hat{v}) + \hat{v}(\dot{\Phi}(\hat{v}) + 2\delta)] & \gamma \\ \gamma^{-1}(\dot{\Psi}(\hat{v}) - \dot{\Phi}(\hat{v}))(\Phi(\hat{v}) + \delta\hat{v})\hat{v} & 0 \end{pmatrix}. \quad (10)$$

Let $A = \Phi(\hat{v}) + \hat{v}(\dot{\Phi}(\hat{v}) + 2\delta)$ and $B = (\dot{\Psi}(\hat{v}) - \dot{\Phi}(\hat{v}))(\Phi(\hat{v}) + \delta\hat{v})\hat{v}$. Then the eigenvalues of matrix (10) are

$$\lambda_{1,2} = \frac{-A \pm \sqrt{A^2 + 4B}}{2}. \quad (11)$$

The biologically important case requires a strictly interior fixed point, which exists only if $\Phi(\hat{v}) + \delta\hat{v} > 0$ and $\hat{v} > 0$. So, I assume these conditions hold. They and the fact that $\dot{\Phi} > 0$ imply that $A > 0$ and that the sign of B is determined by the sign of $\dot{\Psi}(\hat{v}) - \dot{\Phi}(\hat{v})$. From these facts it follows that one eigenvalue of matrix (10), say λ_2 , has a negative real part. The other eigenvalue, λ_1 , depends on the sign of B . If $B > 0 \Leftrightarrow \dot{\Psi}(\hat{v}) > \dot{\Phi}(\hat{v})$, then λ_1 is real and positive, making the fixed point a saddle. If $B < 0 \Leftrightarrow \dot{\Psi}(\hat{v}) < \dot{\Phi}(\hat{v})$, then the real part of λ_1 is always negative, implying local asymptotic stability. The degenerate case, $\dot{\Psi}(\hat{v}) = \dot{\Phi}(\hat{v})$, implying $\lambda_1 = 0$, is unlikely to be important in a biological context, so I will ignore it.

Suppose at least one interior fixed point exists, implying that at least one \hat{v} exists. Also, assume that at every \hat{v} , $\dot{\Phi}(\hat{v}) \neq \dot{\Psi}(\hat{v})$. Since by assumption $\dot{\Phi} > 0$, $\dot{\Psi}$ becomes and stays negative for sufficiently large v , and both Φ and Ψ are continuous, it follows that there must be one equilibrium for which $\dot{\Phi}(\hat{v}) > \dot{\Psi}(\hat{v})$ and no others associated with a larger \hat{v} . Therefore, if any interior fixed points exist, the one corresponding to the largest \hat{v} (the one ‘farthest to the right’ in the phase plane) must be locally asymptotically stable. Because Φ and Ψ are continuous, and given the results in the previous paragraph, if any fixed points exist ‘to the left’ of this right-hand fixed point, then the one with the next lowest \hat{v} must be unstable—a saddle, in fact. And so it continues as we move to the left on the phase plane. If we rank fixed points in order from 1, associated with the largest \hat{v} , to n , associated with the smallest, then points with an odd rank are locally asymptotically stable and even ranks are saddles.

The nontrivial boundary fixed point also participates in this pattern. Consider the n th interior fixed point, associated with the smallest \hat{v} . If it is a saddle, then it must be that $\dot{\Psi}(\hat{v}) > \dot{\Phi}(\hat{v})$. Again, continuity of Φ and Ψ and the fact that $\tilde{v} < \hat{v}$ imply that $\Phi(\tilde{v}) > \Psi(\tilde{v})$. Therefore, given the analysis of matrix (9), the nontrivial boundary fixed point must be locally asymptotically stable. A similar argument shows that if the n th interior fixed point is locally asymptotically stable, then the nontrivial boundary fixed point must be a saddle.

Therefore, on a bifurcation diagram (e.g., Fig. 3) interior fixed points of model (7) typically arise in one of two ways, regardless of which parameter is treated as the bifurcation parameter. They can be born (or die) in pairs by saddle-node bifurcations, or they can pop out of or collide with the non-trivial boundary fixed point. Whenever the latter happens, the boundary equilibrium changes stability. In terms of model (5), this last event is equivalent to a particular solution [see equation (12)] traversing the $y = 0$ boundary and entering the positive cone.

4.2. The biology of models (5) and (7). An interior fixed point of model (7) corresponds to the following solution of model (5):

$$\hat{\phi}(t, x_0) = \begin{pmatrix} \hat{\phi}_x \\ \hat{\phi}_y \\ \hat{\phi}_z \end{pmatrix} = \begin{pmatrix} x_0 e^{\Phi(\hat{v})t} \\ x_0 \hat{v} \gamma^{-1} (\Phi(\hat{v}) + \delta \hat{v}) e^{\Phi(\hat{v})t} \\ x_0 \hat{v} e^{\Phi(\hat{v})t} \end{pmatrix}. \tag{12}$$

The orbit of $\hat{\phi}(t, x_0)$, which I will denote $\hat{\Gamma}(x_0)$, is a ray co-linear with the vector

$$\begin{bmatrix} 1 \\ \hat{v} \gamma^{-1} (\Phi(\hat{v}) + \delta \hat{v}) \\ \hat{v} \end{bmatrix}. \tag{13}$$

Biologically this solution represents a tumor of mass $x(t) = x_0 e^{\Phi(\hat{v})t}$ at time t and initial mass x_0 (Fig. 4). If $\Phi(\hat{v}) \leq 0$ the tumor is regressing or unchanging;

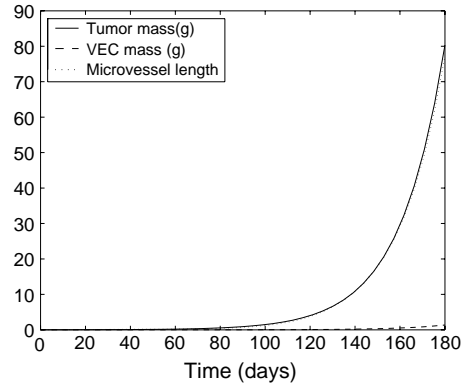


Figure 4. Time evolution of a homogeneous tumor described by model (5) with parameters as in Fig. 2, panels (a) and (b). Initial conditions: $x_0 = 0.1$, $y_0 = 0.001$, $z_0 = 0$.

otherwise it is growing. Along $\phi(t, x_0)$, VEC mass, microvessel length and tumor mass all increase at precisely the same per capita rate.

The nontrivial boundary fixed point represents a regressing tumor with no VECs because $\Phi(\tilde{v}) < 0$ since by definition $\Phi(\tilde{v}) + \delta\tilde{v} = 0$ and by assumption $\delta, \tilde{v} > 0$.

Cases in which no interior fixed points exist, as in panel (f) of Fig. 2, yield the world's most uninteresting tumors. Any such tumor will regress because supporting vasculature can never keep pace with parenchyma. No matter what the initial conditions, since $\max_v \{\Psi(\tilde{v}) - \Phi(v)\} = m < 0$, then $w(t)$ is bounded from above by $w'(t) = w'(0)e^{mt}$, which implies $\lim_{t \rightarrow \infty} w(t) = 0$. Furthermore, v cannot approach 0 with time since \dot{v} becomes positive for sufficiently small w and v . Therefore, $\lim_{t \rightarrow \infty} \dot{v} = -v(\Phi(v) + \delta v)$, implying solutions approach the nontrivial boundary fixed point, producing a tumor that eventually regresses to a state no longer described by the model.

Situations in which only one interior fixed point exists (almost) always produce viable tumors. Numerical investigation of such cases indicate that this fixed point is globally asymptotically stable. Therefore, regardless of the tumor's initial conditions, trajectories eventually approach $\hat{\Gamma}$ and tumor growth rate and composition eventually settle on those described by $\hat{\phi}(t)$.

Transient behavior of solutions approaching an interior fixed point may explain a phenomenon commonly seen in actual tumors: growth rates vary over time, causing tumors to grow in spurts. Traditionally such behavior has been interpreted as parenchyma 'outstripping' its blood supply, its growth rate slowing as a result of lack of blood until microvessel growth catches up. This interpretation is essentially correct in this model, with a couple of subtle new features. First, such irregular growth occurs because of a delay between angiogenesis signal and actual microvessel response. The delay is caused by the time needed to activate and produce new VECs. Second, this model predicts that tumor growth spurts will decrease in amplitude throughout the tumor's life as it approaches its equilibrium growth rate.

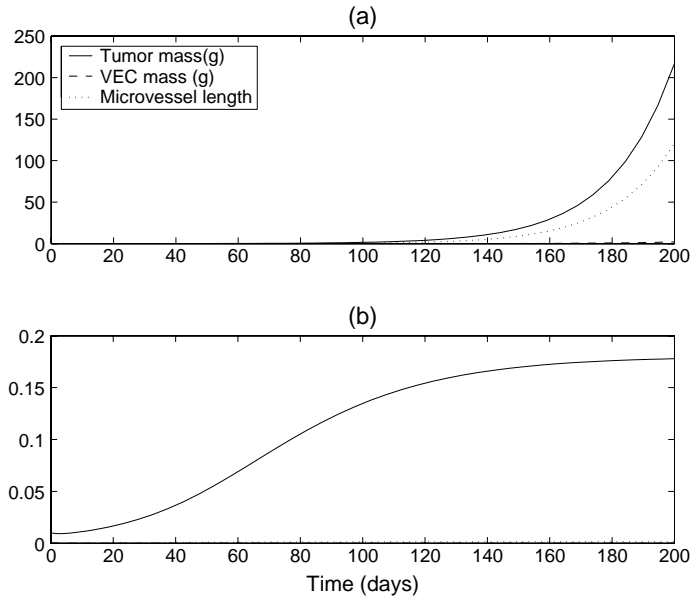


Figure 5. Time evolution of the homogeneous model with parameters as in Fig. 2, panels (c) and (d). Initial tumor mass (x_0) is 0.01 g and initial microvessel density (v_0) is 0. (a) Initial VEC mass (y_0) is 0.001 g ($w_0 = 0.1$). (b) VEC mass starts at 10^{-5} g ($w_0 = 10^{-3}$), below the tumor viability threshold. In this case the tumor eventually dies off.

This conclusion is supported by numerical investigations. In no circumstance has a stable limit cycle been uncovered.

When more than one interior fixed point exists things get more interesting biologically. The model shown in Fig. 2, panels (c) and (d) provides an example (see also Fig. 5). In that instance, the asymptotic behavior of the tumor depends entirely on how well it was initially ‘seeded’ with VECs. The unstable interior fixed point is a saddle with a stable manifold running roughly parallel to the horizontal axis that forms a separatrix (Fig. 6). All solutions starting above this separatrix, corresponding to large w , are attracted to the stable interior equilibrium. The lower region forms the nontrivial boundary equilibrium’s basin of attraction.

Therefore, in this example as in most others studied numerically, initial vascularization does not determine tumor viability. Initial VEC density does. Regardless of initial microvessel density, tumors with VEC density starting too low are destined for extinction. But, any tumor with a sufficiently large initial VEC density is viable. Fig. 5 shows an example.

5. HETEROGENEOUS TUMORS

Here we take up the issue of competition between parenchyma cell types. Imagine a small homogeneous tumor growing as described by solution (12). Suppose

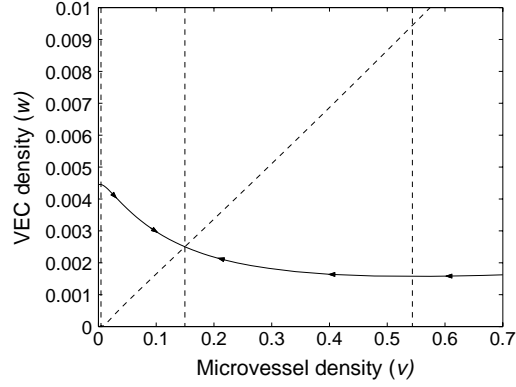


Figure 6. Separatrix (solid curve) for the example in Fig. 2, panels (c) and (d). Dashed curves represent nullclines. Solutions above the separatrix are attracted to the stable interior fixed point; solutions below the separatrix approach the nontrivial boundary equilibrium.

that somewhere in this tumor a single cell mutates into a type 2 cell. It reproduces a few times, creating a small focal population just large enough to be buffered from stochastic events. What is the fate of this mutant population? Will it invade the tumor or decline to extinction? If it invades, will the tumor's clinical aggressiveness be affected? These are the main questions I address with model (1).

One can analyze the heterogeneous model by applying a similar trick to the one used for the homogeneous case. Let $x = x_1 + x_2$, $u_1 = x_1/x$, $u_2 = x_2/x$, $v = z/x$ and $w = y/x$. Differentiating u_1 , u_2 , v and w hands us the following system:

$$\begin{aligned}\frac{du_1}{dt} &= (\Phi_1(v) - \Phi_2(v))u_1u_2 \\ \frac{dv}{dt} &= \gamma w - v(\delta v + \Phi_1(v)u_1 + \Phi_2(v)u_2) \\ \frac{dw}{dt} &= (\alpha H(u_1, v) - \beta - \Phi_1(v)u_1 - \Phi_2(v)u_2)w\end{aligned}\quad (14)$$

$$H(u_1, v) = u_1h_1(v) + u_2h_2(v)$$

$$u_2 = 1 - u_1,$$

with the restriction that $0 < u_1 \leq 1$. This system has all the original fixed points of model (7), namely $(u_1 = 1, v = 0, w = 0)$, $(u_1 = 1, v = \tilde{v}, w = 0)$ where \tilde{v} satisfies $\Phi_1(\tilde{v}) + \delta\tilde{v} = 0$, and $(u_1 = 1, v = \hat{v}, w = \gamma^{-1}\hat{v}[\Phi_1(\hat{v}) + \delta\hat{v}])$, where \hat{v} satisfies $\Psi_1(\hat{v}) = \Phi_1(\hat{v})$. In some circumstances, an additional fixed point occurs at $(u_1 = u^*, v = v^*, w = \gamma^{-1}[\Phi^* + \delta v^*])$, where v^* satisfies $\Phi_1(v^*) = \Phi_2(v^*) \equiv \Phi^*$ and

$$u^* = \frac{\Phi^* - \Psi_2^*}{\Psi_1^* + \Psi_2^*}, \quad (15)$$

with $\Psi_i^* = \alpha h_i(v^*) - \beta$. Since u_1 is restricted to the interval $(0, 1)$, then this last fixed point exists if and only if Φ^* is between Ψ_1^* and Ψ_2^* and $\Phi_1^* + \Phi_2^* \neq 0$. I will ignore the possibility that $(u_1 = u^*, v = v^* = \hat{v}, w = 0)$ since it is not generic and therefore unlikely to be biologically relevant.

PROPOSITION 2. *Suppose a homogeneous tumor consisting (almost) exclusively of type 1 cells is growing along $\hat{\Gamma}$ for some \hat{v} of model (5), and the associated fixed point of model (7) is locally asymptotically stable. Then in the context of the full model (14), this fixed point is unstable if and only if $\Phi_2(\hat{v}) > \Phi_1(\hat{v})$.*

This result follows from the fact that the first row of the Jacobi matrix for any point on the homogeneous tumor boundary is

$$[\Phi_2(\hat{v}) - \Phi_1(\hat{v}) \quad 0 \quad 0], \tag{16}$$

and the lower right 2×2 submatrix of this Jacobian is identical to matrix (10). Therefore, the Jacobi matrix of model (14) has two eigenvalues identical to those of model (7) and one additional eigenvalue equal to $\Phi_2(\hat{v}) - \Phi_1(\hat{v})$, which I will call the ‘invasion eigenvalue’. Since by assumption the first two are strictly less than 0, stability depends only on the sign of the invasion eigenvalue. If $\Phi_2(\hat{v}) > \Phi_1(\hat{v})$, then the invasion eigenvalue is positive and the fixed point is unstable. If the inequality is reversed, the fixed point becomes locally asymptotically stable. Again, I ignore the $\Phi_2(\hat{v}) = \Phi_1(\hat{v})$ case. Biologically, a positive invasion eigenvalue implies that a homogeneous type 1 tumor will be invaded by a small focus of type 2 cells should one arise.

I will not explore all dynamical possibilities of model (14) here. Instead, I confine myself to two important cases: one showing that invasion by an aggressive cell type can destroy a viable tumor; and another suggesting that cell specialization can allow different parenchyma cell types to coexist.

5.1. Selection for an aggressive phenotype can cause necrosis or spontaneous tumor regression. Suppose invading (type 2) cells reproduce more aggressively at every level of perfusion than resident cells (type 1). Suppose further that invaders support their aggressive growth by trading off some of their ability to produce proteins associated with angiogenesis signals. In such a scenario, $\Phi_2(v) > \Phi_1(v)$ and $\Psi_1(v) > \Psi_2(v)$ at every v [Fig. 7(a)].

In this case the mutant type will always invade because the invasion eigenvalue is positive. Numerical investigation suggests that in biologically relevant cases invaders will eventually dominate the tumor (Fig. 8), and perfusion will approach \hat{v}_2 , where \hat{v}_2 satisfies $\Phi_2(\hat{v}_2) = \Psi_2(\hat{v}_2)$ [Fig. 7(c)]. Therefore, tumor per capita growth rate eventually approaches $\Phi_2(\hat{v}_2)$.

How does this invasion affect the tumor’s clinical behavior? If invaders are sufficiently incompetent at enticing blood vessel growth, then $\Phi_2(\hat{v}_2)$ may fall below

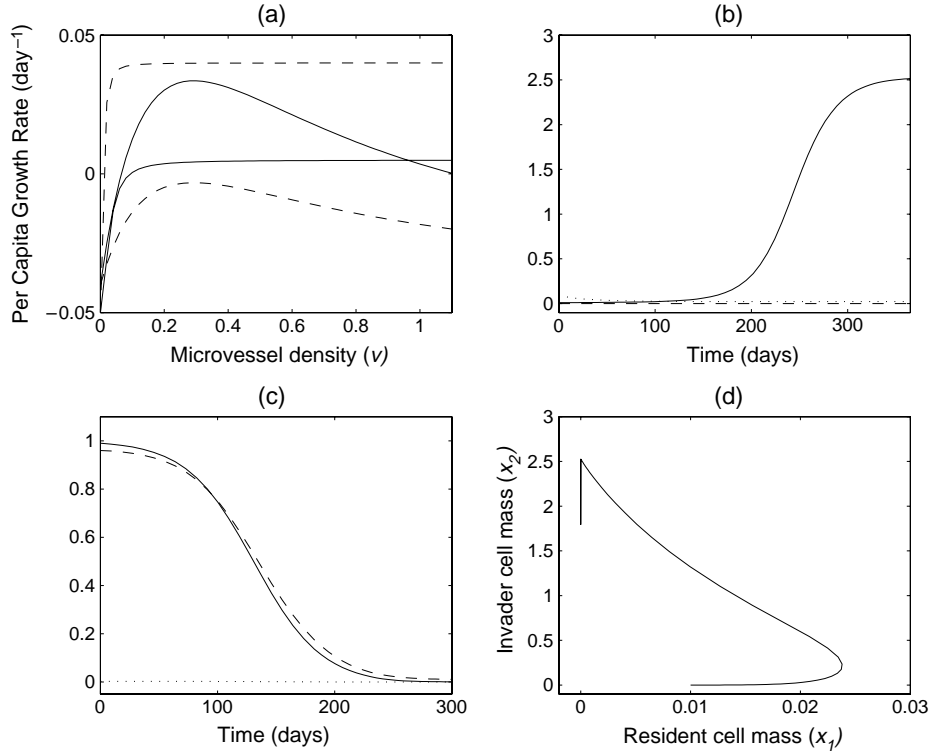


Figure 7. Dynamics of a hypertumor. Parameters for this example (all panels) are the following: for the resident cell type, $A_1 = 0.005$, $B_1 = 0.05$, $\hat{c}_{11} = 0.8$, $\hat{c}_{12} = 3$, $\sigma_1 = 1$, $p = q = 2$, $r_1 = 0.2$, $\xi_1 = 0.06$, $\alpha = 0.06$, $\beta = 0.04$, $\gamma = 3$ and $\delta = 0.004$; for the invader, A_2 is increased to 0.04, r_2 is decreased to 0.1, \hat{c}_{22} is 0.4 and all other parameters are unchanged. (a) Solid lines represent $\Phi_1(v)$ and $\Psi_1(v)$ (resident cell type); dashed lines are $\Phi_2(v)$ and $\Psi_2(v)$ (invader). Invaders reproduce more aggressively at every perfusion, but produce a tiny angiogenesis signal. A homogeneous type 1 tumor is viable, but a homogeneous type 2 tumor is inviable. (b) Time course of a young tumor, from initial vascularization to 1 year old, containing both type 1 and type 2 cells. Initial conditions: $x_1(0) = 0.01$, $x_2(0) = 0.0001$, $y(0) = 2.83 \times 10^{-5}$ and $z(0) = 0.096$. The solid line is tumor mass [$x_1(t) + x_2(t)$, in g], the dotted line is VEC mass [$y(t)$, in mg] and the dashed line is microvessel length ($z(t)$). The tumor stops growing by the end of its first year, reaching a maximum size of about 2.5 g before regressing. (c) Time dynamics of derived variables u_1 (solid line), v (dashed line) and w (dotted line) for the same tumor. Initial conditions: $u_1(0) = 0.99$, $v(0) = 0.96$ and $w(0) = 2.83 \times 10^{-3}$. Transient dynamics have settled by 300 days, by which time the tumor has become dominated by type 2 cells ($u_1 \approx 0$) but is also essentially avascular ($v \approx 0$). (d) Plot of resident cell mass (x_1) vs. invader cell mass (x_2). The tumor moves along this curve counterclockwise with time.

the original tumor's growth rate. Therefore, natural selection favoring a faster-growing parenchyma cell type can paradoxically lead to a slower-growing tumor. In fact, the example in Fig. 7 is even more drastic. Here, $\Phi_2(v_2)$ is negative, and selection eventually causes spontaneous tumor regression. I propose that such a focus of aggressive invaders eventually destroying all or part of a tumor be called a

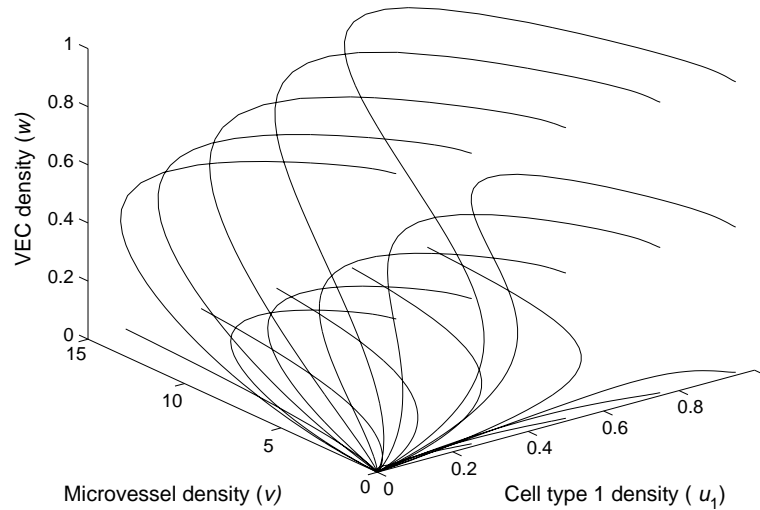


Figure 8. Phase portrait of model (14) for hypertumor example. Parameters are the same as in Fig. 7. In this example, the boundary fixed point appears to be globally asymptotically stable.

hypertumor, in keeping with the analogous concept of a hyperparasite—a parasite living off of another parasite.

5.2. Specialization can allow coexistence of different cell types. In this subsection I change the scenario slightly. Suppose the rare mutant cell type (type 2) is relatively aggressive compared to residents (type 1) when P_{O_2} is moderate to high. However, when P_{O_2} drops below a certain amount, mutant cells trade off their growth advantage for the ability to crank out high levels of tumor angiogenesis factors. In such a scenario, we tend to think of type 1 cells as ‘hypoxic growth specialists’ because they reproduce well under hypoxic conditions, whereas type 2 cells are ‘angiogenesis specialists’ since they produce angiogenesis signals when they are most needed.

Such a scenario can result in a tumor of mixed but stable histology (Figs. 9 and 10). In this situation the two growth functions cross at v^* , and if the tumor can produce an angiogenesis signal allowing the per capita VEC growth rate to exactly match that of the tumor cells (mathematically, Φ^* is between Ψ_1^* and Ψ_2^*), then solutions tend towards the interior fixed point of model (14) according to numerical results. In that case, solutions will approach the trajectory of this solution of model (1):

$$\hat{\psi}(t, x_0) = \begin{pmatrix} \hat{\psi}_{x_1} \\ \hat{\psi}_{x_2} \\ \hat{\psi}_y \\ \hat{\psi}_z \end{pmatrix} = \begin{pmatrix} x_0 e^{\Phi^* t} \\ -x_0 F e^{\Phi^* t} \\ x_0 \gamma^{-1} (v^* + F) (\Phi^* + \delta v^*) e^{\Phi^* t} \\ x_0 (v^* + F) e^{\Phi^* t} \end{pmatrix}, \quad (17)$$

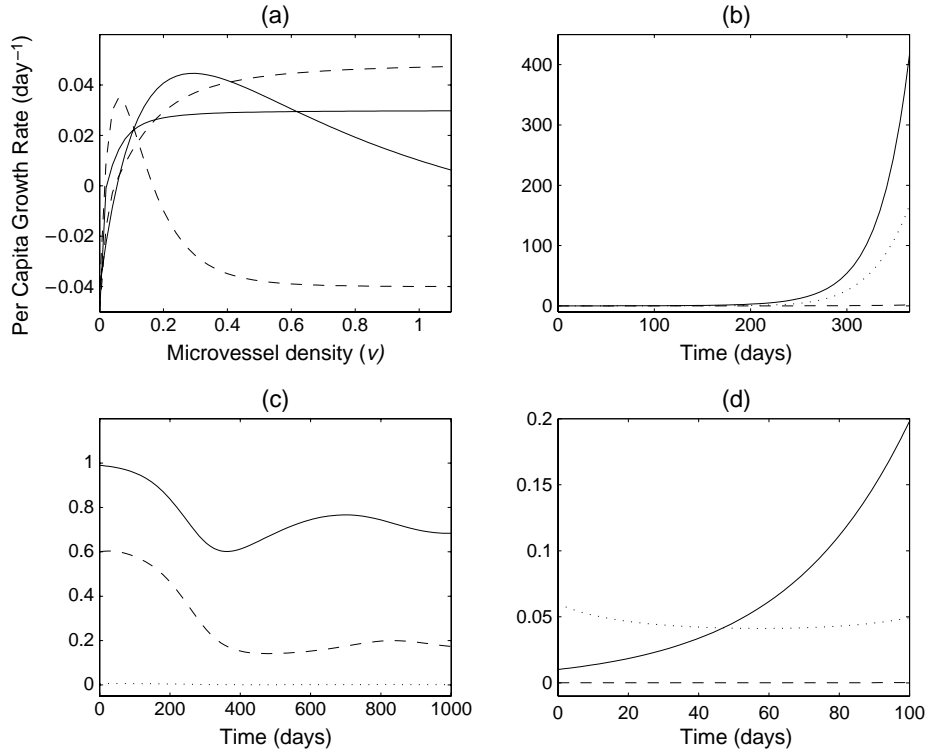


Figure 9. Dynamics of a heterogeneous tumor with stable, mixed histology. Parameters for this example (all panels) are the following: for the resident cell type, $A_1 = 0.03$, $B_1 = 0.05$, $\hat{c}_{11} = 4$, $\hat{c}_{12} = 0.4$, $\sigma_1 = 1$, $p = q = 2$, $r_1 = 0.23$, $\xi_1 = 0.06$, $\alpha = 0.06$, $\beta = 0.04$, $\gamma = 3$ and $\delta = 0.004$; for the invader, A_2 is increased to 0.05, $\hat{c}_{12} = 10$, $\hat{c}_{22} = 1$, $r_2 = 0.85$, $\xi_2 = 0.25$ and all other parameters are unchanged. Therefore, invaders are angiogenesis specialists, and residents are hypoxic growth specialists. (a) Solid lines represent $\Phi_1(v)$ and $\Psi_1(v)$ (resident cell type); dashed lines are $\Phi_2(v)$ and $\Psi_2(v)$ (invader). (b) Time course, from initial vascularization to 1 year of age, of a tumor containing both type 1 and type 2 cells. Initial conditions: $x_1(0) = 0.01$, $x_2(0) = 0.0001$, $y(0) = 6.48 \times 10^{-5}$ and $z(0) = 0.06$. The solid line is tumor mass ($x_1(t) + x_2(t)$, in g), dashed line is VEC mass ($y(t)$, in g) and dotted line is microvessel length ($z(t)$). (c) Time dynamics of proportion of the tumor consisting of type 1 cells (u_1 , solid line), microvessel density (v , dashed line) and VEC density (w , dotted line) for the same tumor, showing very slow decaying oscillations to equilibrium. Initial conditions: $u_1(0) = 0.99$, $v(0) = 0.6$ and $w(0) = 6.48 \times 10^{-3}$. (d) Time dynamics of the same tumor during its first 100 days. Notice that swings in microvessel and VEC densities have just a slight impact on this tumor's growth.

where $x_0 = x_1(0)$ and

$$F = \frac{\Psi_1^* - \Phi^*}{\Psi_2^* - \Phi^*}. \quad (18)$$

Also, the proportion of parenchyma mass consisting of type 1 cells approaches u^* .

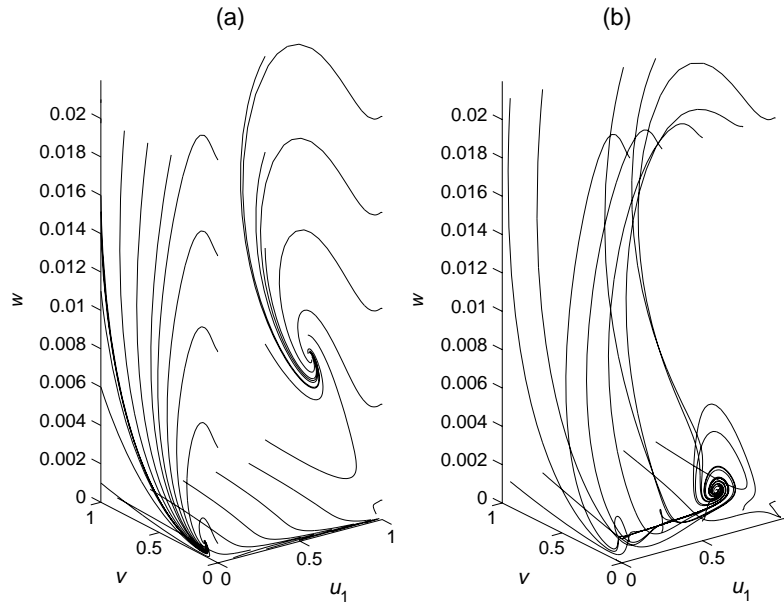


Figure 10. Phase portrait of model (14) for the example in Fig. 9. (a) Dynamics along the boundaries. On the $u_1 = 1$ boundary, most solutions approach the unique interior fixed point for a homogeneous type 1 tumor. Similarly, along the $u_1 = 0$ boundary, solutions approach the unique interior fixed point for a homogeneous type 2 tumor. A mixed tumor starting with no VECs (corresponding to the $w = 0$ boundary) always becomes dominated by type 1 cells, approaching the nontrivial boundary equilibrium for a homogeneous type 1 tumor. Eventually such a tumor decays to extinction. (b) Solutions starting in the interior appear to always approach the interior fixed point corresponding to the point where $\Phi_1(v)$ and $\Phi_2(v)$ cross. In this figure that point is obvious in the lower right portion of the phase space.

6. SUMMARY AND CONCLUSIONS

In this report I present and investigate a mathematical model of single solid tumors assumed to be cancerous. In its most complex setting, the model consists of a system of four nonlinear ordinary differential equations tracking the mass of parenchyma (tumor) cells of up to two different phenotypes, the mass of activated VECs capable of forming new tumor microvessels, and the total length of functional tumor microvessels. With a suitable substitution of variables the number of equations can be reduced by 1, yielding a much simpler model tracking the proportion of the tumor made up of type 1 cells, VEC density and microvessel density. In the simplified model, fixed points correspond to known solutions of the full model. Therefore, I investigate the local stability properties of these solutions, which represent growing or regressing tumors, by analyzing the local stability of fixed points in the lower-dimensional version.

The founding question of this investigation is, what maintains parenchyma cell diversity? In other words, should we view tumors as ecological systems with

competing cell types segregated into distinct niches? Or, is it more insightful to view tumors as integrated tissues, with diverse cell types coordinating their function towards a common goal? Or is it something in between?

The results of this modelling exercise argue for the last possibility—something in between. On one hand, the relationship between parenchyma and stroma resembles tissue integration. In this model, the stroma is represented by immature VECs and mature blood vessels. In both homogeneous and heterogeneous tumor models investigated here, parenchyma and stroma must communicate and coordinate their activities sufficiently to maintain the tumor. If the parenchyma population becomes dominated by incompetent communicators (\hat{v} too low), hypoxia dooms the tumor to extinction. If the stromal population fails to react to the angiogenesis signal with sufficient vigor (α too low), again the tumor succumbs to lack of oxygen.

On the other hand, in no instance did this model show any integration among diverse parenchyma cell types. Such integration would be revealed by a mutualistic relationship among cell types—the tumor would grow more rapidly with a mixture of cell types than it would if it were a homogenous tumor of either cell type. Instead, results always fall into one of two categories. In the first, and in a sense most common, situation one cell type invades and eventually dominates the tumor. Such a situation should be interpreted as competitive exclusion; one cell type is a better competitor and drives the other to extinction.

The second possibility, a mixed, stable histology like that shown in Fig. 9, looks superficially like tissue integration but should be seen as something more like parasitism or incomplete competitive exclusion. The mutant strain is able to invade because, in the environment made by the residents, the mutants are more fit. However, as the mutants become more common, the environment shifts to favor the previous residents more and more until finally the two strains are equally fit and neither has an advantage over the other. However, this situation can occur only when the vascularization where fitnesses become equal (v^*) is between the equilibrium vascularizations of the homogeneous tumors of both types (\hat{v}_1 and \hat{v}_2 , respectively). Therefore, since the growth functions are always monotonically increasing, the mixed tumor will always grow more slowly than a homogeneous tumor of one of the strains in the mix.

Perhaps the most surprising behavior seen in this model is the existence of a ‘hypertumor’, a tiny focus of mutant cells with a selective advantage over resident tumor cells, but with the added property that they kill the tumor by invading it. Their selective advantage arises because they proliferate more rapidly than residents, but they destroy the tumor, and hence themselves, because they are incapable of supporting sufficient angiogenesis to sustain growth.

An important word of caution is required here. Complete tumor destruction by a hypertumor is in fact an artefact caused by a lack of any spatial components within the model. In a more realistic setting, hypertumor cells would remain mostly localized and at most destroy part but rarely all of the tumor. Therefore, a hypertumor

is likely to present itself not as a fully spontaneously regressing tumor but rather as necrosis within the tumor body. One would expect a hypertumor to cause complete regression only in small tumors that can become quickly dominated by the invading hypertumor both numerically and spatially.

Either scenario, necrosis or tumor regression, is highly relevant biologically. Cells are faced with limited resources, so in order for mutation and selection to successfully change a cell's phenotype, certain capabilities must be traded in. Proliferation obviously requires metabolic effort, as does sustained production of angiogenesis signals and growth factors that maintain newly built vessels. It makes sense, therefore, that to produce a viable new phenotype, a mutation increasing a cell's proliferative capacity should do so at the expense of some other capability, possibly the ability to produce angiogenesis growth factors. Note that the possibility of a hypertumor does not require mutations to *always* trade off angiogenesis potential for growth potential, just that it can.

The fact that hypertumors have not been described in the biological literature does not really argue against their existence for two reasons. First, as [Evan and Vousden \(2001\)](#) note in a recent review article, our sample of clinical cancers is highly biased; the only ones we ever see are those that 'beat the odds and appear as clinical disease'. Therefore, we have a very unclear statistical picture of how cancers arise and develop because most are probably never detected.

Ironically, therefore, hypertumors themselves may cause their own rarity since they might be a common cause of spontaneous regression in tiny tumors that never get the chance to manifest themselves clinically. Indeed, the hypertumor hypothesis may explain a well-known oddity in cancer epidemiology again articulated by [Evan and Vousden \(2001\)](#). There are an enormous number of potentially cancerous cells in a single human body relative to the mutation rate, and oncogenic mutations tend to cause altered cells to reproduce many copies of themselves. Therefore, it is quite surprising that viable cancers arise in only about one in three individuals. This surprising situation may in part result from natural selection favoring cancer cell phenotypes that destroy the tumor from within.

The second reason why hypertumors may be undetected is that they may hide in plain sight. As already discussed, in larger tumors a hypertumor might be recognized morphologically as necrosis or a region of apoptosis, a common phenomenon of malignant tumors. The cause of such necrotic or apoptotic regions in larger, vascular tumors is typically explained in textbooks [for example [Cotran et al. \(1999\)](#)] as disruptions in tumor blood supply, often without further explanation of how such disruptions arise. The hypertumor concept represents a mechanistic elaboration of this common hypothesis and increases its power by generating a testable prediction.

If hypertumors exist, then we should find some cancers that evolve a clinically aggressive histology but are paradoxically prone to spontaneous regression. Recent observations made by [Kitanaka et al. \(2002\)](#) suggest that neuroblastoma, a common childhood cancer, may fit this prediction. It appears that the majority of these

cancers are *in situ* lesions, which tend to spontaneously regress (Schofield and Cotran, 1999). Recently, Kitanaka *et al.* (2002) discovered that areas of *in vivo* neuroblastoma tumors undergoing degeneration were characterized by increased expression of *Ras*, a well-known oncogene. Its product is a G-protein active in transducing extracellular growth signals into intracellular signals that upregulate genes involved in cell proliferation. Typically, *Ras* over-expression correlates with more aggressive proliferation (Hannahan and Weinberg, 2000). Kitanaka *et al.* (2002) present evidence that this *Ras*-associated degeneration may in part cause spontaneous regression of neuroblastomas. Therefore, these degenerating areas are candidate hypertumors. However, in their study, Kitanaka *et al.* (2002) generated some features of *Ras*-induced degeneration by transfecting *Ras* into neuroblastoma cells *in vitro* with no vascular infrastructure present. Although this last result does not rule out hypertumors as a cause of spontaneous regression in neuroblastoma, it argues that other molecular events are probably involved.

At first sight it appears that hypertumors may have clinical application if they can be induced. For example, one might 'seed' a tumor with aggressive cells that are incompetent angiogenesis signalers engineered *in vitro*. Alternatively, cells growing within a living tumor may be genetically altered to make them prolific at the expense of growth factor secretion. In either case, induced hypertumors might perhaps damage enough of the primary and established metastatic tumors to at least blunt their growth and invasion of surrounding healthy tissue. Numerical analysis of the models presented in this paper indicate that hypertumors limit overall tumor growth very quickly (Fig. 7); the tumor does not suddenly grow large before dying back.

Nevertheless, certain ecological factors, among other things, argue against hypertumors as therapy. If hypertumors were to be induced, competition for resources within the tumor would become fierce. Such competition coupled with existence of numerous potential colonization sites throughout the host's body would tend to favor dispersive, metastatic phenotypes (Nagy, 1996) leading to much more clinically aggressive disease.

One should view this model as a first approximation to competition among parenchyma cell types within a vascular tumor. The main limitations of the model include a lack of spatial considerations, immune response, multiple competing cell types and larger-scale host/tumor interactions that lead to decelerating tumor growth and patient cachexia. Clearly there is much more to be done. However, models such as this, which view tumors in their ecological and evolutionary context, represent an important but under-explored aspect of cancer biology. For example, we know that natural selection favors cell types that resist both chemo- and radiation therapy, and this selection for resistance is the most common cause of failure in clinical intervention. But, very few if any studies have been performed to determine how one can design natural selection into the treatment instead of hoping to avoid natural selection while implementing the treatment. Ecologically-based mathematical models like those presented here can help fill that void.

ACKNOWLEDGEMENTS

Thanks go to Yang Kuang, Patricia Ashby, Kim Cooper and two anonymous referees for careful and helpful comments. I also thank student collaborators Jason Pattison, Dina Zuber and Natalie Case for literature search and stimulating discussion of the main ideas in this paper.

REFERENCES

- Bertuzzi, A., M. Faretta, A. Gandolfi, C. Sinisgalli, G. Starace, G. Valoti and P. Ubezio (2002). Kinetic heterogeneity of an experimental tumour revealed by BrdUrd incorporation and mathematical modeling. *Bull. Math. Biol.* **64**, 355–384.
- Cahill, D. P., K. W. Kinzler, B. Vogelstein and C. Lengauer (1999). Genetic instability and Darwinian selection in tumors. *Trends Cell Biol.* **9**, M57–M60.
- Carmeliet, P. and R. K. Jain (2000). Angiogenesis in cancer and other diseases. *Nature* **407**, 249–257.
- Chang, C. and Z. Werb (2001). The many faces of metalloproteases: cell growth, invasion, angiogenesis and metastasis. *Trends Cell Biol.* **11**, S37–S43.
- Cheng, K. C. and L. A. Loeb (1997). Genomic stability and instability: a working paradigm. *Curr. Top. Microbiol. Immunol.* **221**, 5–18.
- Colombo, M. P., L. Lombardi, C. Melani, M. Parenza, C. Baroni, L. Ruco and A. Stoppacciaro (1996). Hypoxic tumor cell death and modulation of endothelial adhesion molecules in the regression of granulocyte colony-stimulating factor-transduced tumors. *Am. J. Pathol.* **148**, 473–483.
- Cotran, R. S., V. Kumar and T. Collins (1999). *Pathologic Basis of Disease*, 6th edn, Philadelphia: W.B. Saunders.
- Evan, G. I. and K. H. Vousden (2001). Proliferation, cell cycle and apoptosis in cancer. *Nature* **411**, 342–347.
- Folkman, J., P. Hahnel and L. Hlatky (2000). Cancer: looking outside the genome. *Nat. Rev. Mol. Cell Biol.* **1**, 76–79.
- Gammack, D., H. M. Byrne and C. E. Lewis (2001). Estimating the selective advantage of mutant p53 tumour cells to repeated rounds of hypoxia. *Bull. Math. Biol.* **63**, 135–166.
- Ganong, W. F. (1999). *Review of Medical Physiology*, 19th edn, Stamford, CT: Appleton and Lange.
- Graber, T. G., C. Osmanian, T. Jacks, D. E. Housman, C. J. Koch, S. W. Lowe and A. J. Giaccia (1996). Hypoxia-mediated selection of cells with diminished apoptotic potential in solid tumours. *Nature* **379**, 88–91.
- Hannahan, D. and R. A. Weinberg (2000). The hallmarks of cancer. *Cell* **100**, 57–70.
- Holash, J., P. C. Maisonpierre, D. Compton, P. Boland, C. R. Alexander, D. Zagzag, G. D. Yancopoulos and S. J. Weigand (1998). Vessel cooperation, regression and growth in tumors mediated by angiopoietins and VEGF. *Science* **221**, 1994–1998.
- Horn, L., W. S. Krajewski, P. K. Paul, M. J. Song and M. J. Sydor (1988). Computerized 3-D reconstruction of small blood vessels from high voltage electron-micrographs of thick serial cross sections, in *Vascular Endothelium in Health and Disease*, S. Chien (Ed.), New York: Plenum Press, pp. 35–42.

- Jain, R. K., N. Safabakhsh, A. Sckell, Y. Chen, P. Jiang, L. Benjamin, F. Yuan and E. Keshet (1998). Endothelial cell death, angiogenesis, and microvascular function after castration in an androgen-dependent tumor: role of vascular endothelial growth factor. *Proc. Natl. Acad. Sci.* **95**, 10820–10825.
- Kitanaka, C., K. Kato, I. R. Sakurada, A. Tomiyama *et al.* (2002). Increased *Ras* expression and caspase-independent neuroblastoma cell death: possible mechanism of spontaneous regression. *J. Natl. Cancer Inst.* **94**, 319–321.
- Kraggerud, S. M., J. A. Sandvik and E. O. Pattersen (1995). Regulation of protein synthesis in human cells exposed to extreme hypoxia. *Anticancer Res.* **15**, 683–686.
- Lobov, I. B., P. C. Brooks and R. A. Lang (2002). Angiopoietin-2 displays VEGF-dependent modulation of capillary structure and endothelial cell survival in vivo. *Proc. Natl. Acad. Sci.* **99**, 11205–11210.
- Loeb, L. A. (1996). Many mutations in cancer. *Cancer Surv.* **28**, 329–342.
- Mabry, M., B. Nelkin and S. Baylin (1996). Evolutionary model of lung cancer, in *Lung Cancer: Principles and Practice*, H. I. Pass, J. B. Mitchell, D. H. Johnson and A. T. Turrisi (Eds), Philadelphia, PA: Lippencott-Raven, pp. 133–142.
- Miller, D. L., J. A. Dibbens, A. Damert, W. Risau, M. A. Vadas and G. J. Goodall (1998). The vascular endothelial growth factor mRNA contains an internal ribosome entry site. *FEBS Lett.* **434**, 417–420.
- Nagy, J. D. (1996). Evolutionarily attracting dispersal strategies in vertebrate metapopulations, PhD dissertation, Arizona State University, Tempe, AZ.
- Neufeld, G., T. Cohen, S. Gengrinovitch and Z. Poltorak (1999). Vascular endothelial growth factor (VEGF) and its receptors. *FASEB* **13**, 9–22.
- Qumsiyeh, M. B. and P. Li (2001). Molecular biology of cancer: cytogenetics, in *Cancer: Principles and Practice of Oncology*, V. T. DeVita Jr., S. Hellman and S. A. Rosenberg (Eds), Philadelphia, PA: Lippincott, Williams and Wilkins.
- Rowley, D. R. (1998). What might a stromal response mean to prostate cancer progression? *Cancer Metastasis Rev.* **17**, 411–419.
- Schofield, D. and R. S. Cotran (1999). Diseases of infancy and childhood, in *Pathologic Basis of Disease*, 6th edn, R. S. Cotran, V. Kumar and T. Collins (Eds), Philadelphia, PA: W.B. Saunders, pp. 459–491.
- Stein, I., M. Neeman, D. Shweik, A. Itin and E. Keshet (1995). Stabilization of vascular endothelial growth factor mRNA by hypoxia and hypoglycemia and coregulation with other ischemia-induced genes. *Mol. Cell Biol.* **15**, 5363–5368.
- Terada, T., Y. Okada and Y. Nakanuma (1996). Expression of immunoreactive matrix metalloproteinases and tissue inhibitors of matrix metalloproteinases in human normal livers and primary liver tumors. *Hepatology* **23**, 1341–1344.
- Testa, J. R. (1996). Chromosome alterations in human lung cancer, in *Lung Cancer: Principles and Practice*, H. I. Pass, J. B. Mitchell, D. H. Johnson and A. T. Turrisi (Eds), Philadelphia, PA: Lippencott-Raven, pp. 55–71.
- Thompson, K. E. and J. A. Royds (1999). Hypoxia and reoxygenation: a pressure for mutant p53 cell selection and tumour progression. *Bull. Math. Biol.* **61**, 759–778.
- Tuxhorn, J. A., G. E. Ayala and D. R. Rowley (2001). Reactive stroma in prostate cancer progression. *J. Urol.* **166**, 2472–2483.

- Vajkoczy, P., M. Farhadi, A. Gaumann, R. Heidenreich, R. Erber, A. Wunder, J. C. Tonn, M. D. Menger and G. Breier (2002). Microtumor growth initiates angiogenic sprouting with simultaneous expression of VEGF, VEGF receptor-2, and angiopoietin-2. *J. Clin. Invest.* **109**, 777–785.
- Weibel, E. R. (1984). *The Pathway for Oxygen: Structure and Function of the Mammalian Respiratory System*, Cambridge: Harvard University Press, p. 425.
- Weinert, N. (1997). The multiple roles of tumor stroma. *Virchows Arch.* **430**, 433–443.
- Yancopoulos, G. D., S. Davis, N. W. Gale, J. S. Rudge, S. J. Wiegand and J. Holash (2000). Vascular-specific growth factors and blood vessel formation. *Nature* **407**, 242–248.

Received 21 November 2002 and accepted 10 October 2003